Ann. Geophys., 27, 4075–4087, 2009
www.ann-geophys.net/27/4075/2009/

Annales Geophysicae

Thin embedded current sheets: Cluster observations of ion kinetic structure and analytical models

A. V. Artemyev[1,2], A. A. Petrukovich[1], L. M. Zelenyi[1], R. Nakamura[3], H. V. Malova[1,2], and V. Y. Popov[1,4]

[1]Space Research Institute, Russian Academy of Sciences, Moscow, Russia
[2]Nuclear Physics Institute, Moscow State University, Russia
[3]Space Research Institute, Austrian Academy of Sciences, Graz, Austria
[4]Faculty of Physics, Moscow State University, Russia

Received: 22 June 2009 – Revised: 21 October 2009 – Accepted: 21 October 2009 – Published: 29 October 2009

Abstract. Kinetic structure of embedded thin horizontal current sheets is investigated. Current density estimated by curlometer technique is in general agreement with a sum of electron and proton currents. Embedding of observed thin current sheets in the much wider plasma sheet is apparent in the current density profiles. Ion velocity distributions consist of two parts: the cold non-drifting core likely belongs to the plasma sheet background, while the hotter asymmetric "wings" carry the main portion of the current. Oxygen ions (if present) and higher-energy tails of distribution function can contribute up to 30% of the total current. We compared current density profiles across sheets with three typical current sheet models. Models which allow embedding, describe observed structures equally well at the level of experimental accuracy.

Keywords. Magnetospheric physics (Magnetotail) – Space plasma physics (Numerical simulation studies)

1 Introduction

With the recent four-spacecraft observations in the Earth's magnetotail it is now possible to determine magnetic gradients, electric current densities, to restore (under the condition of stationarity) current density profiles across current sheets (CS) (Runov et al., 2006; Nakamura et al., 2006) as well as to make quantitative comparisons with theory (Sitnov et al., 2006; Baumjohan et al., 2007; Artemyev et al., 2008a). Though some elements of CS structure were described in previous two-spacecraft, or even single-spacecraft experiments, these results substantially relied on lucky occasions and/or limiting suppositions about the sheet geometry and motion. With four points, however, one can investigate CS structure in the full 3-D geometry and on a much larger statistics. For example, CS bifurcation (double-peaked current density) was first reported in GEOTAIL observations by Hoshino et al. (1996). With the recent observations of bifurcated CS by CLUSTER (Sergeev et al., 2003; Runov et al., 2003; Thompson et al., 2006; Israelevich et al., 2008) it became possible to perform thorough comparisons with theories (Zelenyi et al., 2002; Sitnov et al., 2006).

An important result of CLUSTER measurements in the magnetotail is abundance of thin CS (TCS), with the thickness of the order of several ion larmor radii and with very diverse properties (Asano et al., 2005; Petrukovich et al., 2006, 2007; Runov et al., 2006; Nakamura et al., 2006; Baumjohann et al., 2007). Though TCS were observed also earlier by ISEE-1,2 spacecraft (Mitchell et al., 1990; Pulkkinen et al., 1993; Sergeev et al., 1993), their occurrence was not quite clear thus far. In majority of cases current density profiles were distinctly different from the classical Harris shape (Harris, 1962) and were categorized as embedded, bifurcated, or asymmetric (Asano et al., 2005; Runov et al., 2006; Nakamura et al., 2006; Thompson et al., 2006). Another unexpected feature was abundance of strongly tilted (in the YZ GSM plane) sheets with rather variable profiles (Sergeev et al., 2004; Petrukovich et al., 2006), which most likely represent nonstationary structures (Malova et al., 2007; Petrukovich et al., 2008; Zelenyi et al., 2009; Erkaev et al., 2009) and often cannot be explained by motion of the sheet as a whole. A variety of TCS models available now is also quite wide (Kropotkin and Domrin, 1996; Schindler and Birn, 2002; Sitnov et al., 2006; Zelenyi et al., 2004; Yoon and Lui, 2004) (see Sect. 6 for details).

In this report we concentrate on the embedding of TCS (Asano et al., 2005; Runov et al., 2006; Artemyev et al., 2008a). The current density profile of an embedded sheet is substantially narrower, than that of the Harris sheet with the

Correspondence to: A. V. Artemyev
(ante0226@gmail.com)

Published by Copernicus Publications on behalf of the European Geosciences Union.

Table 1. List of current sheet events with smaller peak current density ("slow crossings").

n	date	$<X_{\rm gsm}>$ (1000 km)	$<Y_{\rm gsm}>$	$<Z_{\rm gsm}>$
1	29 Aug 2001: 11:00–11:20	−121	−11	2.5
2	2 Aug 2002: 05:15–05:30	−102	−63	−3.5
3	14 Aug 2002: 03:45–04:00	−113	−40	8.4
4	11 Sep 2002: 11:35–11:55	−116	8	1.1
5	16 Sep 2002: 06:55–07:05	−116	8	1.6
6	2 Oct 2002: 23:50–23:59	−106	53	1.2

same maximum current density. Current density is practically vanishing at some magnetic field $B_x=B_0$, which is distinctly smaller, than the lobe field obtained from the pressure balance $B_{\rm ext}=\sqrt{8\pi n\,(T_i+T_e)}$ (temperature and density values are obtained at CS midplane, where $B_x=0$). Therefore the (background) plasma density is still quite large at $B_x=B_0$ and TCS is embedded in a much thicker plasma sheet. Note, that the current density and plasma pressure profiles of Harris CS (Harris, 1962) are identical and $B_0=B_{\rm ext}$, while at $B_x=B_{\rm ext}/2$ current density is still almost 80% of the maximum. Since a spacecraft is usually crossing TCS in a matter of few minutes (for a thickness of several thousand km and typical flapping velocity of 10-s km/s), and outside it is moving in an almost constant field of a much thicker plasma sheet, observationally B_0 can be also discerned as a maximum of magnetic field in a fast crossing event.

Another important problem of CS structure is a weak correlation between current density measured with the help of the curlometer technique ($\boldsymbol{j}_{\rm curl}=\left(c/4\pi\right)\,{\rm rot}\boldsymbol{B}$) and that obtained from proton flows (Runov et al., 2006; Israelevich et al., 2008). This result (see Sect. 4) contradicts a widespread theoretical assumption that protons are main current carriers and also points out to a presence of some mechanism of currents redistribution.

Using the CS model by Zelenyi et al. (2004), which provides an essential embedding, Artemyev et al. (2008a) have been able to reach an impressing agreement between theoretical and observed current density profiles. However, plasma density and temperature, required by the model to fit the experimental profiles were often rather different (by 30%) from the measured ones. In this report we further elaborate this approach, taking into account the structure of ion distribution function.

The paper is organized as follows. In Sect. 2 we describe the data sources and event selection. In Sect. 3 observed electron and proton currents are compared with curlometer data. In Sects. 4–5 ion component of current is analyzed using distribution functions. In Sect. 6 we review the available TCS models and select three of them for a detailed comparison with experiment. In Sect. 7 we perform comparison with these models.

2 Observational data

Following data from the CLUSTER active archive (CAA) have been used in this work: FGM magnetic field (Balogh et al., 2001), CIS/CODIF moments and velocity distributions (Reme et al., 2001), PEACE electron moments (Owen et al., 2001). The event set for our analysis was mostly adopted from several previous investigations. The fast crossings of 2001, 2003, 2004 were taken from Artemyev et al. (2008a, their Table 1, ## 1–18, 20). Initially they were selected in earlier investigations by Runov et al. (2006) and Nakamura et al. (2006). Eight intervals of prolonged observations of thinning CS were taken from Petrukovich et al. (2007, their Table 1, ## 2, 5, 9, 12, 15, 21, 22, 28). Finally we added six new events with relatively low current densities and thicker sheet (aka "slow" crossings, Table 1).

All selected events are almost horizontal current sheets with relatively small value of B_y ($B_y\sim B_z\ll B_{\rm ext}$). We built the proper coordinate system for each crossing as: normal vector $\boldsymbol{n}$ (almost parallel to $z_{\rm gsm}$ axis, $n_z>0.8$), vector of maximum variation $\boldsymbol{l}$ (close to X, $l_x\sim 1$) and vector $\boldsymbol{m}=[\boldsymbol{l}\times\boldsymbol{n}]$. Curlometer current density $j_{\rm curl}=\left(c/4\pi\right)\,(\boldsymbol{m}\cdot{\rm rot}\boldsymbol{B})$, as well as the coordinate along the normal $z\,(t)-z_0=\int\limits_{t_1}^{t}\partial B_l/\partial t\,[\nabla_n B_l]^{-1}\,dt$ (z_0 is location of CS centre and t_1 is an initial time moment of crossing) are computed with the help of the standard method (see Runov et al., 2006).

Particle current density j was computed as a sum of proton flows, taken from the C-4 and electron flows taken from the C-2, which were interpolated to a common time scale and shifted to allow for different spacecraft positions relative to the magnetic field profile.

3 Comparison between curlometer current density and moments of particle distribution functions

In this section we will perform the comparison between current density derived from the measurements of magnetic field $j_{\rm curl}=\left(c/4\pi\right)\,(\boldsymbol{m}\cdot{\rm rot}\boldsymbol{B})$ and currents computed from electron and ion distribution function measurements as a product of density and Y velocity component (Fig. 1). For each crossing average currents were determined for the central part of CS ($\langle B_l\rangle_{sc}<5$ nT) ($\langle...\rangle_{sc}$ denotes averaging over available four CLUSTER spacecraft). Following the event classification (Sect. 2) in Fig. 1 we mark fast crossings from 2001, 2004 (spacecraft separation about 1000–2000 km), fast crossings from 2003 (spacecraft separation about 300 km), events of thinning CS and relatively thick sheets ("slow" crossings, from 2001, 2002). $j_{\rm curl}$ and j_p are only weakly correlated, proton current is always smaller than the required one and is sometimes negative, while curlometer current is always positive, as it should be for a cross- magnetotail current (Fig. 1a). This result agrees with the similar earlier

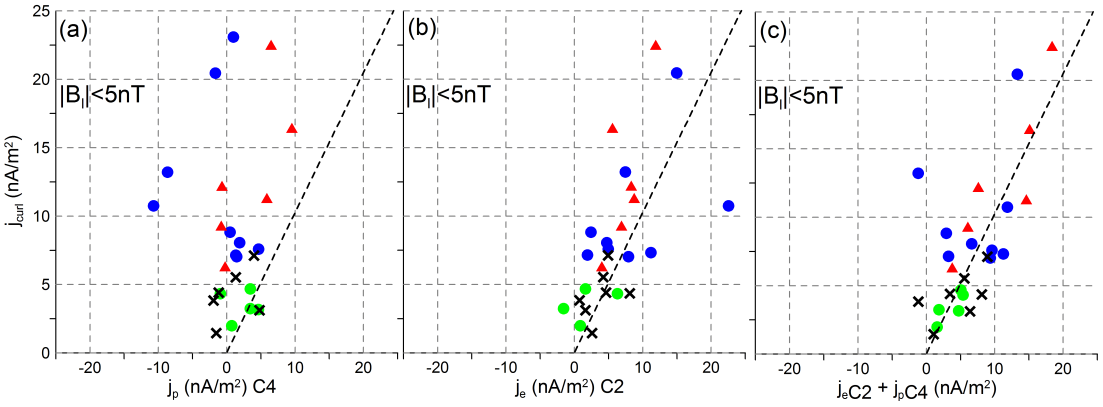

Fig. 1. Comparison of current density $j_{\rm curl}$ with proton and electron currents. Current density is averaged over central region of CS $\langle B_l \rangle_{sc}$ <5 nT. Following symbols are used: blue circles -for fast crossings from 2001 and 2004, green circles – for slow crossings from Table 1, red triangles – for fast crossings from 2003 and crosses – for thinning CS. Dashed line corresponds to $j_{\rm particle}=j_{\rm curl}$.

findings for bifurcated CS (Israelevich et al., 2008) and thin CS (Runov et al., 2006). Electron currents are always positive and generally better correspond to $j_{\rm curl}$ (Fig. 1b), especially for higher current densities. Addition of electron currents practically eliminates the shift to negative values in proton currents and improves correlation with $j_{\rm curl}$ (Fig. 1c).

Despite the general statistical agreement, curlometer and particle currents may differ substantially for some events. Another difficult issue is a balance of electron and proton contributions to current. Though the models described in Sect. 6 have a possibility to manipulate with electron currents, the major component is still expected to be the proton one. Cases with negative or very small proton currents thus can not be now straightforwardly interpreted. Ion bulk velocity related to diamagnetic drift and quasi-adiabatic motion should be much larger than electron bulk velocity (in the system without electric field). To explain the dominant electron current one can use the assumption about particle cross field drift (Asano et al., 2004; Israelevich et al., 2008). It means that coordinate system in which CS does not move has some velocity in negative direction.

Due to small value of such electric field in quiet conditions it can not be directly measured. In this case the balance between electron and ion currents could be used for determination of the coordinate system in which the comparison between theory and observation could be carried out. For the detailed analysis we choose in this investigation several events with substantial proton current and good agreement between particle current and $j_{\rm curl}$. Therefore we try to analyze the ion velocity distribution structure in the system close to one without a drift (without electric field).

4 Proton currents and distribution functions

In this section we will study the kinetic structure of a proton component of TCS currents. For this purpose we are choosing two crossings with substantial proton currents for which full cross-sheet profiles are available (Figs. 2 and 3). The comparison of curlometer current density with the proton and electron currents (averaged over 16 s) is shown in these figures. In addition we also calculate the "partial" proton current, carried by protons with energies higher than $E_{\rm min}$.

$$j_p = \frac{1}{2} e \int f_p \sin 2\theta \sin\varphi d\theta d\varphi \int_{E_{\rm min}}^{E_{\rm max}} E dE \qquad (1)$$

Varying the minimum energy $E_{\rm min}$ one can determine the relative importance of the core and wings of the velocity distribution. Figures 2 and 3 include such partial current density for $E_{\rm min} \sim 2/3 T_p$ with the cold core removed. The curves of partial and total current practically coincide in both events, and therefore the most of the current is carried by hot wings of ion distribution.

This bimodal structure is further investigated in velocity distributions (Figs. 4 and 5) averaged over the time intervals shown in Figs. 2 and 3 by thin vertical lines. The right "wings" of 1-D velocity distributions (Figs. 4a and 5a) are indeed noticeably higher than the left ones and this effect is responsible for the bulk of the current. Such a function cannot be approximated by a single shifted maxwellian distribution, because the shift along v_y grows with the increase of energy (not shown here). This asymmetry is well manifested in 2-D distribution (Figs. 4b and 5b) as a broken ring structure. A part of distribution with $E<E_{\rm min}$ ($E_{\rm min}$=5 keV for Fig. 4 and $E_{\rm min}$=2 keV for Fig. 5) is removed from these 2-D plots to increase the visibility.

For the given energy range (in CODIF instrument) distributions are reasonably well approximated by two maxwellian functions with different temperatures (Table 2). The most of the current is carried by the hotter component with substantial drift velocity, forming wings, while the colder core has much lower drift velocity, which could be even of the

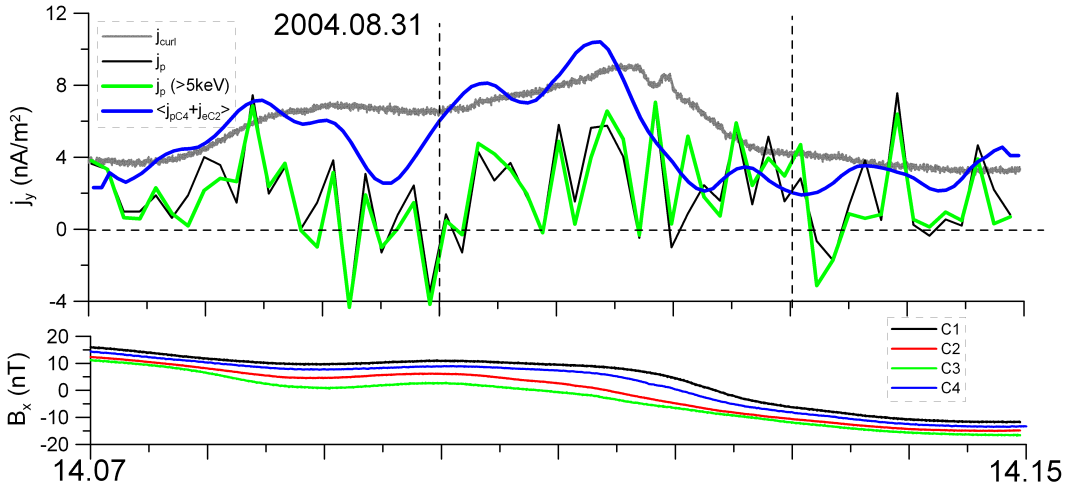

Fig. 2. Crossing of thin CS detected on 31 August 2004. Top panel: curlometer current density (grey curve) compared with particle currents (see text for details). Bottom panel: B_x magnetic field.

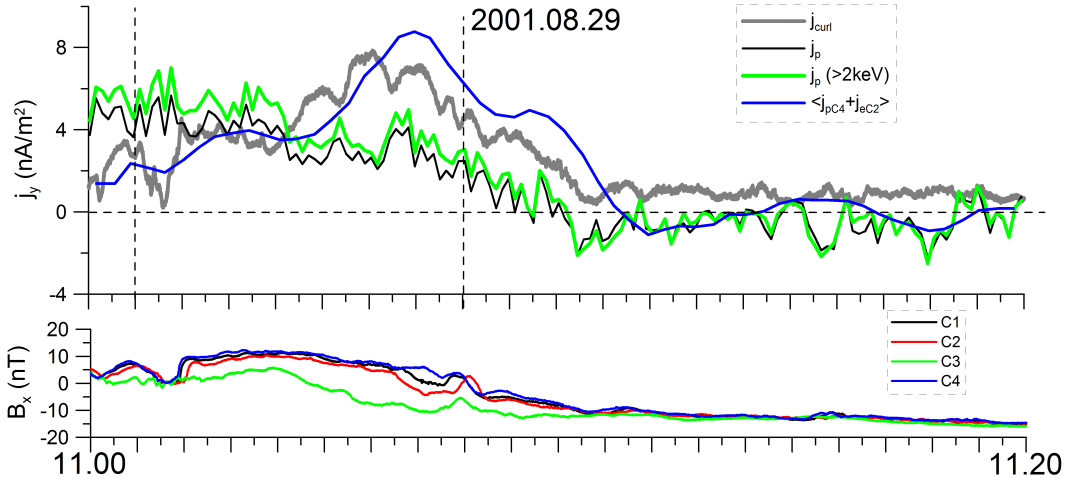

Fig. 3. The same as Fig. 2 but for 8 August 2001.

different sign (for the crossing shown in Fig. 2) . Densities of cold and hot components are comparable. Therefore up to 50–70% of particle density (the whole cold component) in these cases could be interpreted as another population of plasma differing from current carriers (here it is called background plasma). Of course, a part of the hotter component might also belong to background plasma and density of current-carrying particles could be overestimated.

5 Currents of heavy ions and high-energy particles

The real space plasmas may contain several ion species, in particular O^+, which can carry current also. Indeed for a current sheet crossing (from 11 September 2002, Fig. 6) with 25% presence of O^+, oxygen ions carry a substantial part of current and their velocity distribution has asymmetric "wings" too (Fig. 7a, b), which are even more pronounced than the proton ones.

Since current-carrying ions are located at the edges of distribution as it is measured by the CIS/CODIF CLUSTER instrument, it is reasonable to estimate the part of current, which could be carried by ions with energies beyond the device energy range. Such extrapolation is presented in Fig. 7 (for three studied crossings, including one with oxygen ions). Power law function $f_i \sim v_y^{\tau}$ was used for extrapolation up to 100 keV, τ was determined taking five or two last points of velocity distributions in CODIF range (shown by two different markers). Both measured and approximated number and current densities are also shown in these plots. When temperature is high: $T_p \sim 7-9$ keV (event 31 August 2004), up to $\sim$30% of ion current can be left unaccounted for, depending on the extrapolation law. For crossing 29 August 2001 where

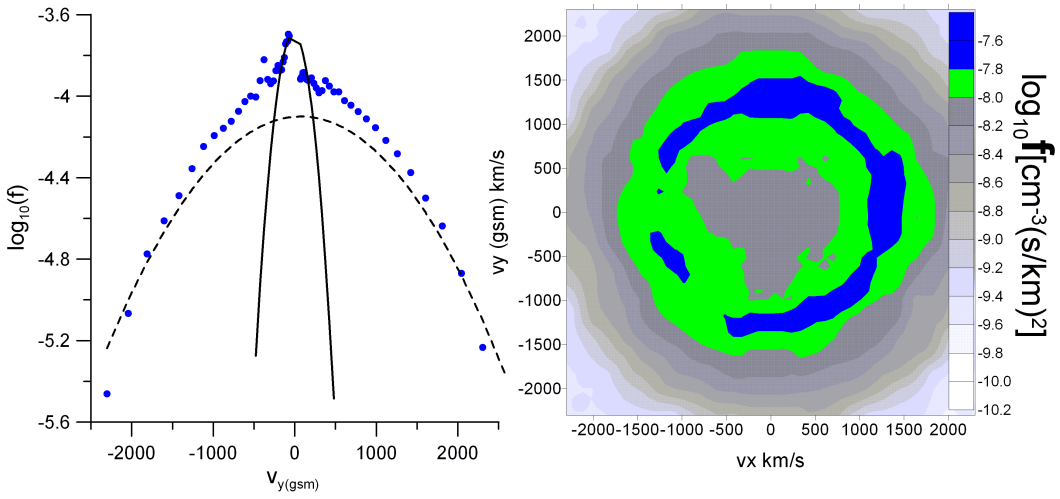

Fig. 4. Event 31 August 2004. Left: 1-D proton velocity distribution (blue points) and maxwellian approximations for central core (black line), and "wings" (dashed line). Right: 2-D proton velocity distribution obtained by integration along v_z for all particles with $E>5$ kev. Color scale is selected to highlight asymmetry of distribution wings.

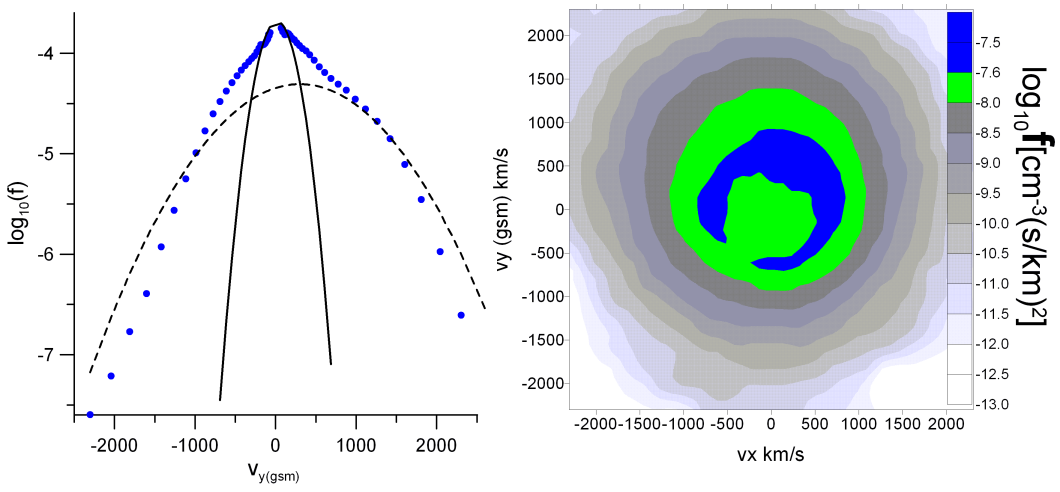

Fig. 5. The same as Fig. 4, but for event 29 August 2001 (cut-off energy $E>2$ kev for the right plot).

protons have low temperature ($T_p \sim 3$ keV) such extrapolation practically does not add any additional current. Substantial part of the oxygen current (30%) can also be missed at higher energies (for event 11 September 2002).

6 Models of current sheet

Several important features of observed current sheets should be incorporated in any model, attempting to describe real data. First of all, the models under discussion should be able to reproduce the embedding of current sheets into much broader plasma sheet, so that plasma pressure at CS edges (where current density has sufficiently small value) is still essential. The second crucial feature is a finite normal magnetic field component B_n, which has a dramatic influence on particle dynamics (Buechner and Zelenyi, 1989). So, we are looking for the stationary equilibrium CS model with $B_n \neq 0$.

Keeping in mind these requirements, we choose several available models for the comparison with experiment. The first model is the generalization of the classical Harris CS model (Harris, 1962), which was designed by Yoon and Lui (2004) (hereinafter referred to as YL2004). This model can be considered as a modification of an earlier model (Zelenyi and Krasnoselskikh, 1979). The ratio of particle drift velocity $v_{Dp}/|v_{De}|=U$ is a free parameter and velocity distribution is given as a sum of shifted and nonshifted maxwellians (with densities n_0 and n_0' correspondingly). Embedding in YL2004 is determined by the parameter $\delta=n_0'/n_0$. The presence of the B_n in CS requires the establishing of pressure

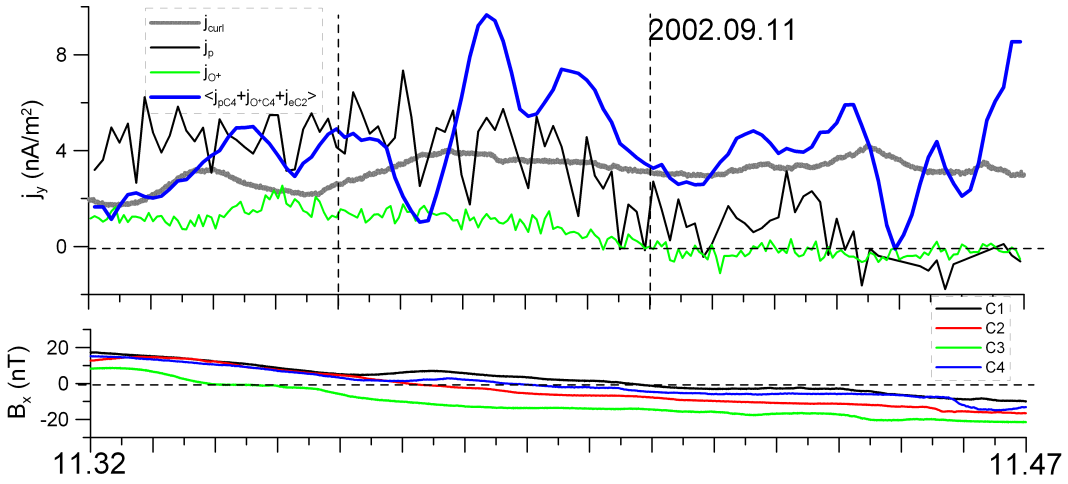

Fig. 6. Crossing of thin CS detected on 9 September 2002 with oxygen current. Top panel: curlometer current density (grey curve) compared with particle currents (see text for details). Bottom panel: B_x magnetic field.

Table 2. Parameters of two maxwellians fitted to observed proton velocity distribution.

data	core				Wings				total	
	n cm^{-3}	u km/s	T keV	j nA/m^2	n cm^{-3}	u km/s	T keV	j nA/m^2	n cm^{-3}	T keV
31 Aug 2004: 14:10–14:13	0.1	−15	0.3	−0.25	0.21	100	11	3.2	0.31	8.2
29 Aug 2001: 11:00–11:08	0.1	20	0.3	0.3	0.09	300	5.4	4.8	0.19	3.0

balance along XZ-direction. In YL2004 it could be done by introducing a slow gradient along x-coordinate (Kan, 1973; Voronina and Kan, 1993).

The second model that we adopt, is a modification of a thin CS model (Schindler and Birn, 2002 – hereinafter referred to as SB2002), which is constructed using more general class of velocity distributions with specific dependence on the canonical moment (see for detail Schindler and Birn, 2002; Birn et al., 2004). The problem of the stress balance in the presence of the finite B_n could be solved again taking into account some spatial gradient along x. However, if we want to study the 1-D configuration, this gradient can be chosen by hand, so that the value of B_n is equal to the observed one. The ratio of electron and proton currents is controlled by the model parameters (see for details Schindler and Birn, 2002). The embedding is achieved by inclusion of the additional term to velocity distribution – the nonshifted maxwelian distribution with density n_0'. The ratio n_0'/n_0 determines the relative fraction of the background plasma density (this option with $n_0' \neq 0$ hereafter is referred to as SB2002*).

The third model we use is a thin anisotropic CS model (Zelenyi et al., 2004) with electron component (hereafter referred to as TACS). It can be also considered as a generalization of some earlier models of thin CS (Eastwood, 1972; Kropotkin and Domrin, 1996). The ion component of TACS was found taking into account conservation of the quasi-adiabatic invariant $I_z = \oint v_z dz$. Such an approach is valid for equilibriums with $B_n \leq 0.2 B_0$. Here we assume that CS is thin enough and could assume that equilibrium is exactly 1-D (but $B_n \neq 0$), so $\partial B_n / \partial x \equiv 0$. For the electron component the guiding-center approach was used. The ratio of proton and electron currents can be adjusted by parameter $b_n = B_n / B_0$. TACS embedding is controlled by the ratio of thermal and a flow velocities $\varepsilon = v_T / v_D$ at the edges of CS (Burkhart et al., 1992; Artemyev et al., 2008a).

7 Comparison of observations and models of thin CS

Comparison of observed CS with three above specified models is carried out in this section. As a first step we approximated experimental profiles following the Artemyev et al. (2008a) approach, using the measurements of total proton density and temperature (proton velocity distribution is integrated with $E_{\min}=0$). The approximation is based on parameters B_0, B_{ext}, n_p, T_p, T_e, j_0 (j_0 is maximum value of j_{curl}). We tried to find the suitable model (parameters) by minimizing the following function $R(M)$:

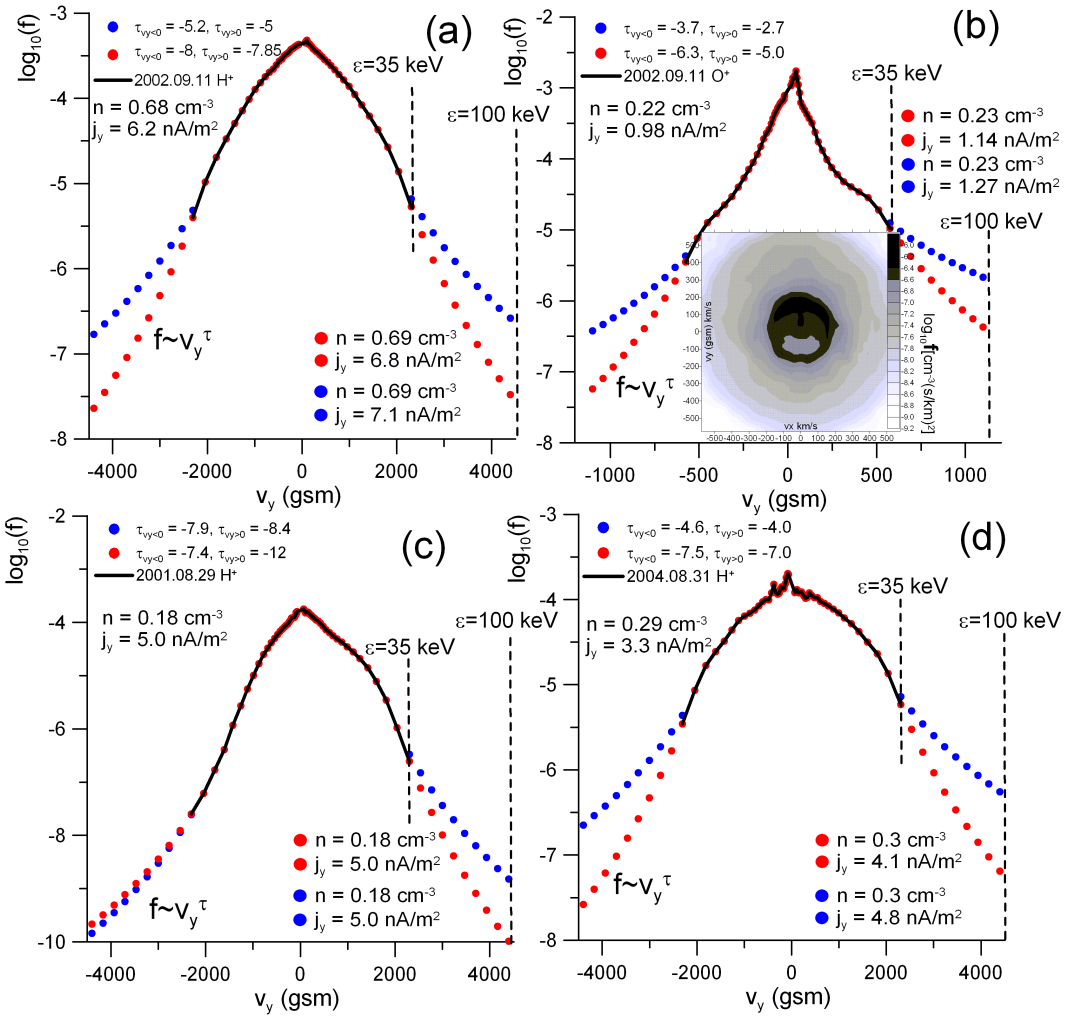

Fig. 7. Observed CIS/CODIF ion velocity distribution functions (black curves) with extrapolation obtained by using two (red circles) and five (blue circles) last points. The text on panels includes parameters of extrapolation $f \sim v_y^{-\tau}$, CIS/CODIF number and current densities, as well as their extrapolated values.

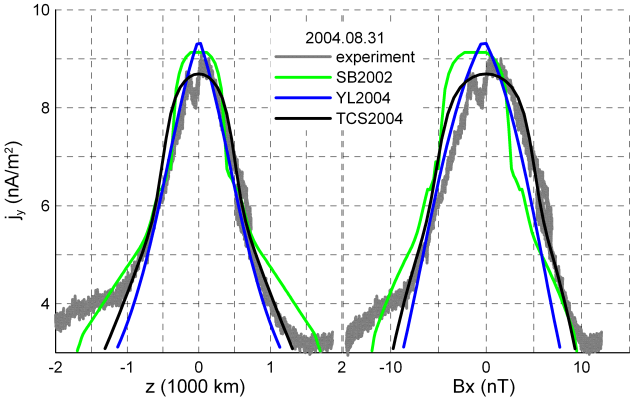

Fig. 8. Comparison of current density profiles for event 31 August 2004.

$$R^2(M) = \left(1 - B_{\text{ext}}^{(M)} \Big/ B_{\text{ext}}\right)^2 + \left(1 - B_0^{(M)} \Big/ B_0\right)^2 + \left(1 - j_0^{(M)} \Big/ j_0\right)^2 + \left(1 - T_e^{(M)} \Big/ T_e\right)^2 + \left(1 - n_p^{(M)} \Big/ n_p\right)^2 + \left(1 - T_p^{(M)} \Big/ T_p\right)^2 \quad (2)$$

Model parameters are with the superscript (M), experimental parameters – without superscripts. The priority was given to better coincidence of the maximum current density (the value of function $\left(1 - j_0^{(M)} \Big/ j_0\right)^2$ is set to be not more than 0.05).

In order to adapt models to a finite spatial resolution of the Cluster tetrahedron, theoretical current density profiles were smoothed out by a sliding window, corresponding to

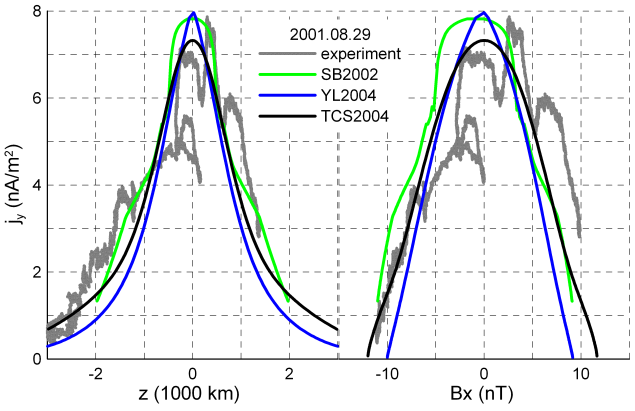

Fig. 9. Comparison of current density profiles for event 29 August 2001.

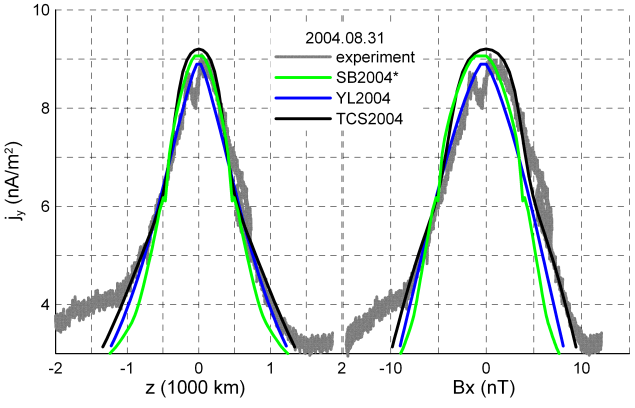

Fig. 10. Comparison of current density profiles for event 31 August 2004. Only current-carrying plasma component is taken (see text for details).

spacecraft separation ∼1000 km (for 2001 and 2004). Experimental curlometer profiles as a function of spatial coordinate are built as explained in Sect. 2 and paper by Runov et al. (2006). Input parameters of the models are: proton temperature, electron temperature, and B_0. We use parameter B_z/B_0 as input only for TACS model, because in YL2004 and SB2002 models value of B_z is controlled only by a spatial gradient $\partial/\partial x$, which can not be determined from our observations. Model plasma density was determined using the pressure balance. Model profiles of current density were obtained self-consistently. Input parameters of the models were varied in the vicinity of experimental ones to achieve a better coincidence of theoretical current density profiles with observations (see Artemyev et al., 2008a, for details).

The model and observed current density profiles as functions of spatial coordinate and magnetic field are shown in Figs. 8 and 9 for two crossings described in Sect. 5. All three models used for the comparison approximate observed profiles reasonably well. However, comparison between model

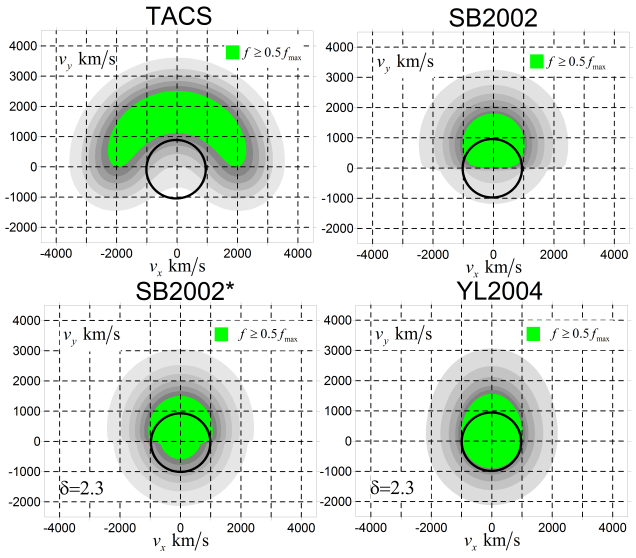

Fig. 11. Velocity distribution of protons for models of CS. The color scale highlights asymmetry of hot wings. Black circles mark energy 5 keV.

and experimental parameters (density, temperature, B_0, B_{ext} and estimate of CS thickness $L_0 \sim (c/4\pi)\, B_0/j_0$, Tables 3 and 4) reveals certain differences between the models. Both experimental crossings are approximated equally well only by YL2004, which has free parameter δ (ratio of background and current-carrying plasma densities). Using δ one can adjust easily the value B_{ext}/B_0. TACS model has also the possibility to regulate the value of B_{ext}/B_0 with the help of parameter ε, but this mechanism is not so flexible, because ε affects CS thickness as well. Nevertheless, TACS model describes observations with only 30% error (see Artemyev et al., 2008a, for more examples). The worst is the model SB2002, which can not regulate embedding and plasma density in SB2002 model is substantially smaller than the observed one.

Now we continue comparison of YL2004, TACS and SB2002* models for one observation (event 31 August 2004), but will use only plasma density and temperature of current-carrying plasma (hot wings, from Table 2) as an input (Fig. 10, to be compared with Fig. 8). All three models again approximate observations reasonably well. Note that the pressure of excluded cold plasma is less than 10% of the total one and thus removing of this part practically does not change static balance. But now model and observed plasma parameters are practically equal (Table 5, to be compared with Table 3). Here SB2002* model, allowing the embedding was used in this comparison instead of SB2002.

Thereby, one could conclude that for better comparison with experiment models should have some relatively free parameter for regulating their embedding (as was noticed in Sect. 6), while model velocity distributions should have

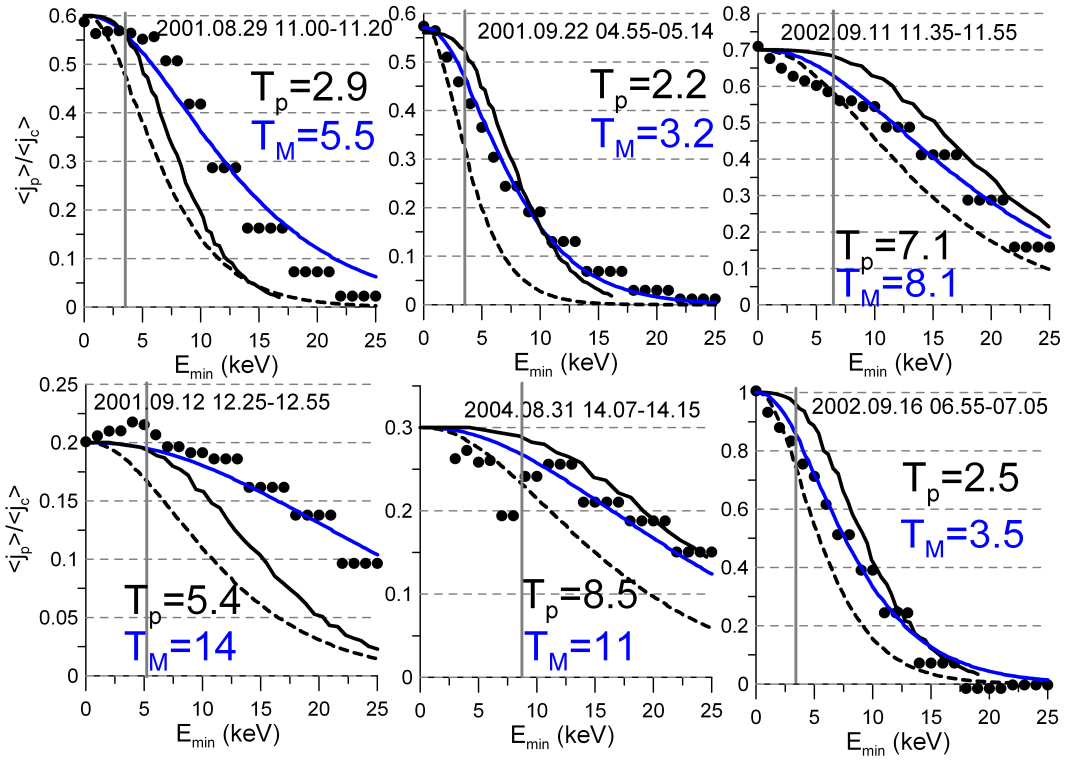

Fig. 12. Observed ratio $\langle j_p \rangle / \langle j_{\rm curl} \rangle$ as a function of minimum integration energy for six events (black points). The expected ratio for a single maxwellian distribution with the observed temperature T_p (dashed curve). The expected ratio for distribution from TACS model with temperature T_p (black curve). The best fit maxwelian distribution with temperature T_M (grey curve).

Table 3. Comparison with models for event 31 August 2004.

	B_0, nT	$B_{\rm ext}$, nT	n, cm^{-3}	T_p, keV	T_e, keV	j_0, nA/m^2	L_0, 10^3 km
exp	15(−15)	35	0.31	8.2	2.2	9.1	1.3
SB2002	13(−13)	17	0.09	6.0	1.5	9.1	1.1
TACS	13(−13)	25	0.12	6.4	1.6	8.5	1.2
YL2004	13(−13)	32	0.25	8.0	2.0	9.3	1.1

asymmetric "wings", carrying the bulk of the current. The central region of the model velocity space generally could be filled by the background plasma (in the case of approximation of CS as a whole with background) or could be empty (in a case of approximation of current carriers only). All three models used above have such hot asymmetric "wings". The model distribution functions are presented in Fig. 11. The central region (here $E<5$ keV, shown with black circles) could be cut out without substantial current density decrease.

Finally we confirm our conclusions by the analysis of proton distribution functions obtained during several crossings (including two described above) with a substantial proton current (two cases have been chosen from a set of thinning CS and other two – from the Table 1). For each event the ratio $\langle j_p \rangle / \langle j_{\rm curl} \rangle$ was computed as a function of a low limit of integration energy $E_{\rm min}$ (Fig. 12, dotted curves) (velocity distribution functions were averaged over the central sheet where $\langle B_l \rangle_{sc} < 5$ nT). Observed proton temperatures T_p are shown by thin vertical lines and printed at each panel. Indeed, proton current density does not decrease substantially, until $E_{\rm min} < T_p$ in agreement with the presence of a hot current-carrying component. Further we attempted to approximate the observed $\langle j_p \rangle / \langle j_{\rm curl} \rangle$ with the simple model distribution functions. The current produced by a single maxwellian function with the temperature T_p (dashed curves) is always decreasing faster than observations. A single maxwellian may fit only if it's temperature T_M (shown in panels) is higher than the observed one. Proton distributions taken from the TACS model with the temperature T_p fit observations relatively well (solid black curves in Fig. 12). Therefore one

Table 4. Comparison with models for event 29 August 2001.

	B_0, nT	B_{ext}, nT	n, cm^{-3}	T_p, keV	T_e, keV	j_0, nA/m^2	L_0, 10^3 km
exp	10(−15)	20	0.19	3.0	1.1	7.9	1.2
SB2002	11(−11)	14	0.1	3.0	1.2	7.8	1.1
TACS	10(−10)	20	0.20	3.0	0.8	7.3	1.0
YL2004	12(−12)	18	0.20	3.0	1.0	8.0	1.1

Table 5. Comparison with models for event 31 August 2004. Only current-carrying plasma component is taken (see text for details).

	B_0, nT	B_{ext}, nT	n, cm^{-3}	T_p, keV	T_e, keV	j_0, nA/m^2	L_0, 10^3 km
exp	15(−15)	30	0.21	11	2.2	9.1	1.3
SB2002*	12(−12)	29	0.18	11	2.0	9.1	1.0
TACS	14(−14)	31	0.19	10.6	2.1	9.2	1.2
YL2004	13(−13)	30	0.18	11	2.2	8.9	1.1

can conclude that the current is formed either by hot shifted maxwelian distribution with the temperature larger than the observed one or by protons with the complex velocity distribution structure (like in TACS model).

8 Discussion

With the comprehensive Cluster multi-point measurements of magnetic field, ion and electron moments and ion distribution functions in the magnetotail, we performed a detailed comparison of embedded current sheets with several typical theoretical models. Only horizontal thin current sheets observed in quiet conditions with single peaked current density profiles well resolved by curlometer were used in the analysis.

The embedding of thin intense current sheets in a much wider plasma sheet with much smaller current density was confirmed by ion distribution function analysis. The current is transported mainly by hot wings of proton distribution function (in Cluster case, measured by CIS/CODIF up to 40 keV). A smaller part of the current could be transported by protons above 40 keV (in case of higher temperature) and/or oxygen ions. Cold ions (with energy is roughly about 1 keV) do not carry noticeable current and thus form the plasma population probably belonging to the embedding plasma sheet. The scale of this plasma sheet is supposed to be much larger than the typical CLUSTER separation and therefore corresponding magnetic gradients are generally not well resolved by the spacecraft tetrahedron.

Ion distribution functions were often studied for active events with bursty bulk flows (Nakamura et al., 1991; Raj et al., 2002), as well as generally in the plasma sheet or PSBL (Eastman et al., 1984; Elphic and Gary, 1990). However such specific analysis in TCS has not been carried out so far. Recently Zhou et al. (2009) reported about similar features in the structure of ion distribution function, observed by THEMIS.

Taking for comparison only current-carrying component of proton distribution functions helps to improve substantially the degree of conformity between of experimental and theoretical profiles and plasma moments. All three models used (SB2002*, YL2004, TACS) have almost an equally good agreement with analyzed CLUSTER observations. However, it should be mentioned that two models discussed above (SB2002*, YL2004) require a finite gradient $\partial/\partial x \neq 0$ to support finite $B_z \neq 0$. In this paper we analyzed only the vertical cuts of the model plasma configurations (i.e. for x=const). And therefore to prove the model applicability in the vicinity of observed CS one needs also to make an additional comparison of $\partial/\partial x$ and B_z, which is currently impossible with available dataset. TACS model assumes $\partial/\partial x \sim 0$ and if the observed CS is thin and stretched enough ($\partial/\partial x \ll B_z/B_0 \partial/\partial z$) the model is valid in some domain along the Sun-Earth line (x-direction).

However for CLUSTER with its relatively small satellite separation measurements of gradients in x-direction will not be of any practical use. For such quasi 1-D configurations the models differ only in modifications of particle distribution function. However since the distribution of the current-carrying protons can not be clearly separated from the plasma population, which does not carried any current, it's properties like anisotropy and non-gyrotropy are hard to resolve in the experimental data. In particular Cully et al. (2006) reported about absence of specific anisotropy of plasma pressure (predicted by TACS) in CLUSTER data.

In a given energy range (below 40 keV) distribution functions with the reasonable accuracy can be fitted with two

shifted Maxwellians. However, it is important to consider rather wide energy range (in case of high temperature to add also energetic particle measurements) when computing currents from ion and electron flows. Since distribution functions with power law energy tails are common in the magnetotail (see also Vasyliunas, 1968; Christon et al., 1989), using CS models with kappa distribution functions (Fu and Hau, 2005; Yoon et al., 2006) might be also of interest in future. In this paper we obtain the ion distribution functions with non-Maxwellian velocity tails with power laws $\tau\sim-3$ to -8 ($\log_{10} f_i\sim\tau \log_{10} v_y$). For the respective energy distributions kappa is then less than 5 ($f\sim\varepsilon^{-\kappa-1}$, $\kappa=1-\tau/2$).

Embedding geometry has a quite substantial effect on stability due to increasing free energy of CS (Zelenyi et al., 2008; Zelenyi et al., 2009, and references therein). For the kink instability in Harris CS Karimabadi et al. (2003) have shown that growth rate increases and real part of frequency decreases with addition of background plasmas. Similar result has been obtained for TACS model (Artemyev et al., 2008b). Therefore observations of CS oscillations (Sergeev et al., 2004; Petrukovich et al., 2006) with frequencies much lower than theoretical predictions for CS without any background could be related right with the presence of background plasma.

Finally we want to make one more substantial remark for a future study. In many experimental cases electron current dominates over proton current. However, in the models electron properties are substantially less restricted by observable parameters, than the proton ones. Therefore for the analysis of embedding presented above we have taken only sheets with substantial proton currents. The problem of electron currents needs it is own study.

Comparison between current density determined with the help of curlometer technique and that computed as a sum of proton and electron flows shows the general agreement of two quantities, both for the statistics of averaged values and for the time profiles for specific cases. However, in agreement with the previous investigations $j_{\rm curl}$ and proton current are only weakly correlated (Runov et al., 2006; Israelevich et al., 2008). One could conclude that there exists some mechanism of decreasing proton current and increasing electron one, while preserving the total current. This mechanism might be quite different from the mechanisms of the total current formation. The latter can be due to pressure gradient $j_{DM}\sim dp/dz$, paramagnetic effect of open trajectories of "Speiser" ions, as well as due to gradient drifts $j_{GR}\sim dB_l/dz$. On the other hand the general eastward plasma drift with v_0 velocity decrease proton current ($j_p\rightarrow j_p-en_pv_0$) and increase electron one ($j_e\rightarrow j_e+en_pv_0$), keeping total current unchanged.

The velocity $-v_0\boldsymbol{e}_y$ of plasma could be supported by $E_z=-\left(v_0/c\right)B^2/B_x$ or by $E_x=\left(v_0/c\right)B^2/B_z$. E_z is taken into account by many CS models. In case of absence of normal magnetic field B_z one can use the balance between ion and electron current to determine the E_z (see for example Yoon and Lui, 2004). However the vertical profile of velocity E_zB_x/B^2 is essentially inhomogeneous because $E_z\sim0$ and $B_x\sim0$ near the center of CS. In addition, in the presence of the B_z electric field E_z can not support any particle drift in the center region of CS: $E_zB_x/B^2=0$ in $z=0$.

Therefore it is more logical to consider E_xB_z/B^2 as a main source of hidden plasma drift. First of all, component of magnetic field B_z is likely almost uniform across thin CS. Secondly, since $B_z\ll B_0$, a very small and unobservable $E_x\sim0.05\,\mathrm{mV/m}$ is sufficient to produce the required shift of velocities $v_0\sim100\,\mathrm{km/s}$ in the center of CS (where $v_0\sim E_x/B_z$). It is impossible to calculate E_x in the frame of modern CS models, since most of them belong to the class of 1-D or quasi 1-D equilibriums. However, such field with the correct sign (Earthward pointing) was detected in the laboratory experiment (Minami et al., 1993). Also some estimates of E_x have been done by taking into account averaged particle bulk velocity with connection CS evolution around substorm onset (Asano et al., 2004).

9 Conclusions

Thin quiet horizontal current sheets, observed by Cluster are shown to be essentially embedded in a much thicker plasma sheet and thus could be considered as a special plasma configuration. In consistency with the embedding of electric current, ion velocity distributions in CS contain two parts: cold non-drifting core, likely belonging to the plasma sheet background and hot asymmetric "wings", carrying the current. Density of these current-carrying particles could be substantially smaller than total plasma density. A number of models, having sufficient flexibility to incorporate the embedding, could conform with observations with similar accuracy. To make further distinction of models one needs to measure $\partial/\partial x$ gradient in the current sheet or to reveal details in velocity distribution of current carriers. For YL2004 and SB2002 models gradient $\partial/\partial x$ should have specified values to match the experiment, while for TACS model the only requirement is that the gradient $\partial/\partial x$ should be small enough.

In the future electron currents need to be studied in more detail, to explain that the ratio of electron and proton currents could differ very significantly from case to case, while models usually predict the dominance of ion current. One such candidate mechanism might be an electric field drift in the direction opposite to direction of total current.

Acknowledgements. Authors would like to acknowledge Cluster Active Archive and Cluster instrument teams, in particular FGM, CIS, PEACE for excellent data. This work was supported in part by the RF Presidential Program for State Support of Leading Scientific Schools (project no. NSh-472.2008.2), the Russian Foundation for Basic Research (project nos. 08-02-00407, 09-05-00410). A.A.V. would like to acknowledge hospitality of IWF.

Topical Editor I. A. Daglis thanks V. A. Sergeev and another anonymous referee for their help in evaluating this paper.

References

Artemyev, A. V., Petrukovich, A. A., Zelenyi, L. M., Malova, H. V., Popov, V. Y., Nakamura, R., Runov, A., and Apatenkov, S.: Comparison of multi-point measurements of current sheet structure and analytical models, Ann. Geophys., 26, 2749–2758, 2008a, http://www.ann-geophys.net/26/2749/2008/.

Artemyev, A. V., Zelenyi, L. M., Malova, Kh. V., and Popov, V. Yu.: Effect of the normal component of the magnetic field on the kink instability of the Earth's magnetospheric current sheet, Plasma Physics Report, 34(9), 771–779, 2008b.

Asano, Y., Mukai, T., Hoshino, M., Saito, Y., Hayakawa, H., and Nagai, T.: Statistical study of thin current sheet evolution around substorm onset, J. Geophys. Res., 109, A05213, doi:10.1029/2004JA010413, 2004.

Asano, Y., Nakamura, R., Baumjohann, W., Runov, A., Voros, Z., Volwerk, M., Zhang, T. L., Balogh, A., Klecker, B., and Reme, H.: How typical are atypical current sheets?, Geophys. Res. Lett., 32(3), L03108, doi:10.1029/2004GL021834, 2005.

Balogh, A., Carr, C. M., Acuña, M. H., Dunlop, M. W., Beek, T. J., Brown, P., Fornacon, K.-H., Georgescu, E., Glassmeier, K.-H., Harris, J., Musmann, G., Oddy, T., and Schwingenschuh, K.: The Cluster Magnetic Field Investigation: overview of in-flight performance and initial results, Ann. Geophys., 19, 1207–1217, 2001, http://www.ann-geophys.net/19/1207/2001/.

Baumjohann, W., Roux, A., Le Contel, O., Nakamura, R., Birn, J., Hoshino, M., Lui, A. T. Y., Owen, C. J., Sauvaud, J.-A., Vaivads, A., Fontaine, D., and Runov, A.: Dynamics of thin current sheets: Cluster observations, Ann. Geophys., 25, 1365–1389, 2007, http://www.ann-geophys.net/25/1365/2007/.

Birn, J., Schindler, K., and Hesse, M.: Thin electron current sheets and their relation to auroral potentials, J. Geophys. Res., 109(A2), A02217, doi:10.1029/2003JA010303, 2004.

Buechner, J. and Zelenyi, L. M.: Regular and chaotic charged particle motion in magnetotaillike field reversals 1. Basic theory of trapped motion, J. Geophys. Res., 94(A9), 11812–11842, 1989.

Burkhart, G. R., Drake, J. F., Dusenbery, P. B., and Speiser, T. W.: A particle model for magnetotail neutral sheet equilibria, J. Geophys. Res., 97(A9), 13799–13815, 1992.

Christon, S. P., Williams, D. J., Mitchell, D. G., Frank, L. A., and Huang, C. Y.: Spectral characteristics of plasma sheet ion and electron populations during undisturbed geomagnetic conditions, J. Geophys. Res., 94, 13409–13424, 1989.

Cully, C. M., Ergun, R. E., Lucek, E., Eriksson, A., Baker, D. N., and Mouikis, C.: Forced current sheets in a flapping magnetotail, Int. Conf. Substorms, 8, 43–48, 2006.

Eastman, E. T., Frank, L. A., Peterson, W. K., and Lennartsson, W.: The plasma sheet boundary layer, J. Geophys. Res., 89(A3), 1553–1572, 1984.

Eastwood, J. W.: Consistency of fields and particle motion in the 'Speiser' model of the current sheet, Planet. Space Sci., 20, 1555–1568, 1972.

Elphic, E. C. and Gary, S. P.: ISEE observation of low frequency waves and ion distribution function evolution in the plasma sheet boundary layer, Geophys. Res. Lett., 17(11), 2023–2026, 1990.

Erkaev, N. V., Semenov, V. S., Kubyshkin, I. V., Kubyshkina, M. V., and Biernat, H. K.: MHD aspect of current sheet oscillations related to magnetic field gradients, Ann. Geophys., 27, 417–425, 2009, http://www.ann-geophys.net/27/417/2009/.

Fu, W.-Z. and Hau, L.-N.: Vlasov-Maxwell equilibrium solutions for Harris sheet magnetic field with Kappa velocity distribution, Phys. Plasmas, 12(7), 070701-070701-4, 2005.

Harris, E. G.: On a plasma sheet separating regions of oppositely directed magnetic field, Nuovo Cimento, 23, 115–121, 1962.

Hoshino, M., Nishida, A., Mukai, T., Saito, Y., Yamamoto, T., and Kokubun, S.: Structure of plasma sheet in magnetotail: Doublepeaked electric current sheet, J. Geophys. Res., 101, 24775–24786, 1996.

Israelevich, P. L., Ershkovich, A. I., and Oran, R.: Current carriers in the bifurcated tail current sheet: Ions or electrons?, J. Geophys. Res., 113(A4), A04215, doi:10.1029/2007JA012541, 2008.

Kan, J. R.: On the structure of the magnetotail current sheet, J. Geophys. Res., 78, 3773–3781, 1973.

Karimabadi, H., Daughton, W., Pritchett, P. L., and Krauss-Varban, D.: Ion-ion kink instability in the magnetotail: 1. Linear theory, J. Geophys. Res., 108(A11), 1400, doi:10.1029/2003JA010026, 2003.

Kropotkin, A. P. and Domrin, V. I.: Theory of a thin one-dimensional current sheet in collisionless space plasma, J. Geophys. Res., 101(A9), 19893–19902, 1996.

Malova, H. V., Zelenyi, L. M., Popov, V. Y., Delcourt, D. C., Petrukovich, A. A., and Runov, A. V.: Asymmetric thin current sheets in the Earth's magnetotail, Geophys. Res. Lett., 34, L16108, doi:10.1029/2007GL030011, 2007.

Minami, S., Podgornyi, A. I., and Podgornyi, I. M.: Laboratory evidence of earthward electric field in the magnetotail current sheet, Geophys. Res. Lett., 20(1), 9–12, 1993.

Mitchell, D. G., Williams, G. J., Huang, C. Y., Frank, L. A., and Russell, C. T.: Current carriers in the near-Earth cross-tail current sheet during substorm growth phase, Geophys. Res. Lett., 17, 583–586, 1990.

Nakamura, M., Paschmann, G., Baumjohann, W., and Sckopke, N.: Ion distribution and flows near the neutral sheet, J. Geophys. Res., 96(A4), 5631–5649, 1991.

Nakamura, R., Baumjohann, W., Runov, A., and Asano, Y.: Thin current sheets in the magnetotail observed by Cluster, Space Sci. Rev., 122, 29–38, 2006.

Owen, C. J., Fazakerley, A. N., Carter, P. J., Coates, A. J., Krauklis, I. C., Szita, S., Taylor, M. G. G. T., Travnicek, P., Watson, G., Wilson, R. J., Balogh, A., and Dunlop, M. W.: Cluster PEACE observations of electrons during magnetospheric flux transfer events, Ann. Geophys., 19, 1509–1522, 2001, http://www.ann-geophys.net/19/1509/2001/.

Rème, H., Aoustin, C., Bosqued, J. M., et al.: First multispacecraft ion measurements in and near the Earths magnetosphere with the identical Cluster ion spectrometry (CIS) experiment, Ann. Geophys., 19, 1303–1354, 2001, http://www.ann-geophys.net/19/1303/2001/.

Petrukovich, A. A., Zhang, T. l., Baumjohann, W., Nakamura, R., Runov, A., Balogh, A., and Carr, C.: Oscillatory magnetic flux tube slippage in the plasma sheet, Ann. Geophys., 24, 1695–1704, 2006,

http://www.ann-geophys.net/24/1695/2006/.

Petrukovich, A. A., Baumjohann, W., Nakamura, R., Runov, A., Balogh, A., and Rème, H.: Thinning and stretching of the plasma sheet, J. Geophys. Res., 112(A10), A10213, doi:10.1029/2007JA012349, 2007.

Petrukovich, A. A., Baumjohann, W., Nakamura, R., and Runov, A.: Formation of current density profile in tilted current sheets, Ann. Geophys., 26, 3669–3676, 2008, http://www.ann-geophys.net/26/3669/2008/.

Pulkkinen, T. I., Baker, D. N., Owen, C. J., Gosling, J. T., and Murthy, N.: Thin current sheets in the Deep Geomagnetotail, Geophys. Res. Lett., 20, 2427–2430, 1993.

Raj, A., Phan, R., Lin, R. P., and Angelopoulos, V.: Wind survey of high-speed bulk flows and field-aligned beams in the near Earth plasma sheet, J. Geophys. Res., 107, 1419, doi:10.1029/2001JA007547, 2002.

Runov, A., Nakamura, R., Baumjohann, W., Zhang, T. L., Volwerk, M., Eichelberger, H.-U., and Balogh, A.: Cluster observation of a bifurcated current sheet, Geophys. Res. Lett., 30, 1036, doi:10.1029/2002GL016136, 2003.

Runov, A., Sergeev, V. A., Nakamura, R., Baumjohann, W., Apatenkov, S., Asano, Y., Takada, T., Volwerk, M., Vörös, Z., Zhang, T. L., Sauvaud, J.-A., Rème, H., and Balogh, A.: Local structure of the magnetotail current sheet: 2001 Cluster observations, Ann. Geophys., 24, 247–262, 2006, http://www.ann-geophys.net/24/247/2006/.

Schindler, K. and Birn, J.: Model of two-dimensional embedded thin current sheets from Vlasov theory, J. Geophys. Res., 107(A8), 1193, doi:10.1029/2001JA000304, 2002.

Sergeev, V. A., Mitchell, D. G., Russell, C. T., and Williams, D. J.: Structure of the tail plasma/current sheet at 11 Re and its changes in the course of a substorm. J. Geophys. Res., 98, 17345–17365, 1993.

Sergeev, V., Runov, A., Baumjohann, W., Nakamura, R., Zhang, T. L., Volwerk, M., Balogh, A., Reme, H., Sauvaud, J. A., Andre, M., and Klecker, B.: Current sheet flapping motion and structure observed by Cluster, Geophys. Res. Lett., 30(6), 1327, doi:10.1029/2002GL016500, 2003.

Sergeev, V., Runov, A., Baumjohann, W., Nakamura, R., Zhang, T. L., Balogh, A., Louarnd, P., Sauvaud, J.-A., and Reme, H.: Orientation and propagation of current sheet oscillations, Geophys. Res. Lett., 31(5), L05807, doi:10.1029/2003GL019346, 2004.

Sitnov, M. I., Swisdak, M., Guzdar, P. N., and Runov, A.: Structure and dynamics of a new class of thin current sheets, J. Geophys. Res., 111(A8), A08204, doi:10.1029/2005JA011517, 2006.

Thompson, S. M., Kivelson, M. G., El-Alaoui, M., Balogh, A., Reme, H., and Kistler, L. M.: Bifurcated current sheets: Statistics from Cluster magnetometer measurements, J. Geophys. Res., 111, A03212, doi:10.1029/2005JA011009, 2006.

Vasyliunas, V. M.: A Survey of Low-Energy Electrons in the Evening Sector of the Magnetosphere with OGO 1 and OGO 3, J. Geophys. Res., 73, 2839–2884, 1968.

Voronina, V. A. and Kan, J. R.: A kinetic model of the plasma sheet - Isotropic nonuniform plasma temperature, J. Geophys. Res., 98(A8), 13395–13402, 1993.

Yoon, P. H. and Lui, A. T. Y.: Model of ion- or electron-dominated current sheet, J. Geophys. Res., 109(A11), A11213, doi:10.1029/2004JA010555, 2004.

Yoon, P. H., Lui, A. T. Y., and Sheldon, R. B.: On the current sheet model with κ distribution, Phys. Plasmas, 13(10), 102108–102108-6, 2006.

Zelenyi, L. M. and Krasnoselskikh, V. V.: Relativistic Modes of Tearing Instability in a Background Plasma, Soviet Astronomy (tr. Astr. Zhurn.), 23, 460–467, 1979.

Zelenyi, L. M., Delcourt, D. C., Malova, H. V., and Sharma, A. S.: "Aging" of the magnetotail thin current sheets, Geophys. Res. Lett., 29(12), L05105, doi:10.1029/2001GL013789, 2002.

Zelenyi, L. M., Malova, H. V., Popov, V. Yu., Delcourt, D., and Sharma, A. S.: Nonlinear equilibrium structure of thin currents sheets: influence of electron pressure anisotropy, Nonlin. Processes Geophys., 11, 579–587, 2004, http://www.nonlin-processes-geophys.net/11/579/2004/.

Zelenyi, L., Artemyev, A., Malova, H., and Popov, V.: Marginal stability of thin current sheets in the Earth's magnetotail, J. Atmos. Solar-Terr. Phys., 70, 325–333, 2008.

Zelenyi, L. M., Artemyev, A. V., Petrukovich, A. A., Nakamura, R., Malova, H. V., and Popov, V. Y.: Low frequency eigenmodes of thin anisotropic current sheets and Cluster observations, Ann. Geophys., 27, 861–868, 2009, http://www.ann-geophys.net/27/861/2009/.

Zhou, X.-Z., Angelopoulos, V., Runov, A., Sitnov, M. I., Coroniti, F., Pritchett, P., Pu, Z. Y., Zong, Q.-G., McFadden, J. P., Larson, D., and Glassmeier, K.-H.: Thin current sheet in the substorm late growth phase: Modeling of THEMIS observations, J. Geophys. Res., 114, A03223, doi:10.1029/2008JA013777, 2009.